HMT 3760 10 January 2003 Disk used ARTICLE IN PRESS No. of Pages 10, DTD = 4.3.1 SPS, Chennai

Available online at www.sciencedirect.com
SCIENCE DIRECT®

PERGAMON

International Journal of Heat and Mass Transfer xxx (2003) xxx–xxx

International Journal of HEAT and MASS TRANSFER

www.elsevier.com/locate/ijhmt

Natural convective heat transfer from isothermal cuboids

Ewa Radziemska, Witold M. Lewandowski *

Department of Apparatus and Chemical Machinery, Gdansk University of Technology ul. G. Narutowicza 11/12, 80-952 Gdańsk, Poland

Abstract

The paper presents results of theoretical and experimental investigations of the convective heat transfer from isothermal cuboid. The analytical solution was performed taking into account complete boundary layer length and the manner of its propagation around isothermal cuboid. It arises at horizontal bottom surface and grows on vertical lateral surface of the block. After changing its direction, the boundary layer occurs above horizontal surface faced up and next it is transformed into buoyant convective plume. To verify obtained theoretical solution the experimental study has been performed. The experiment was carried out for three possible positions of tested the same cuboid.

As the characteristic linear dimension in Nusselt–Rayleigh theoretical and experimental correlations we proposed the ratio of six volumes to the cuboids surface area, for the analogy to the same ratio using as the characteristic dimension for the sphere, which is equal to the sphere's diameter. It allowed performing the experimental results independently from the orientation of the block. The Rayleigh numbers based on this characteristic length ranged from 10^5 to 10^7. The Nusselt number describing intensity of convective heat transfer from the cuboid can be expressed by: $Nu = XRa^{1/5} + YRa^{1/4}$, where X and Y are coefficients dependent on the cuboid's dimensions. For the range of provided experiment the experimental Nusselt–Rayleigh relation can be presented in the form:

$$Nu = 1.61Ra^{1/5} \text{ or } 0.807Ra^{1/4}$$

with the good agreement with the theoretical one recalculated for the tested cuboid dimensions.

1. Introduction

Free convective heat transfer, especially from bodies or objects limited by cuboids surfaces, take place in building engineering, central heating, electronics, aeronautics, aquanauts, chemical apparatus, lighting industry. In these branches cubes are very often used as insulating, constructing or shielding surfaces.

The mechanism of heat transfer considered from all surfaces of cuboid is more complicated then from flat horizontal or vertical plates treated separately. The boundary layer from downward faced bottom of the cuboid has the significant influence on the formation of boundary layer on vertical side and next on boundary layer above horizontal top of the block. Up to now these configurations of surfaces (horizontal flat plates facing downward [1–4], horizontal flat plates facing upward [5–11] and vertical plates [1,9,12]) have been studied theoretically and experimentally independently. In the case of cuboids we found significantly less papers devoted them. Culham et al. [13] proposed three analytical models presented for determining laminar and forced convection heat transfer from isothermal cuboids. It is a convenient method for calculating an average Nusselt number, base on cuboid dimensions, thermophysical properties and the approach velocity. Cha and Cha [14] presented the numerical and experimental investigations results of 3D natural convection flows around two interacting isothermal cubes. Yovanovich [15] compared models of Chamberlain, Stretton and Clemes for cube and cuboid and also Karagiosis and Saunders model for vertical plate in microelectronic heat sink applications. Meinders et al. [16] provided experiments of the local

* Corresponding author. Tel.: +48-58-347-24-10/18-74; fax: +48-58-347-24-58/18-74.

E-mail address: ewarad@chem.pg.gda.pl (W.M. Lewandowski).

0017-9310/02/$ - see front matter © 2002 Published by Elsevier Science Ltd.
doi:10.1016/S0017-9310(02)00533-1

Nomenclature

$a = \frac{\lambda}{C_p}\rho$	thermal diffusivity (m^2/s)
a	width of the cuboid (m)
A	control surface across the boundary layer (m^2)
b	length of the cuboid (m)
c	height of the cuboid (m)
C	$Nu(Ra)$ relation constant (–) (Eq. (33))
c_p	specific heat at constant pressure (J/(kg K))
dS	control surface of heated surface (m^2)
F	surface of the cuboid (m^2)
g	acceleration due to gravity (m/s^2)
i	enthalpy (J/kg)
I	electric current (A)
L	characteristic length (m)
n	$Nu(Ra)$ relation exponent (–) (Eq. (33))
$Nu = \frac{\alpha L}{\lambda}$	Nusselt number (–)
$Pr = \nu/a$	Prandtl number (–)
$\dot{Q}$	heat flux (W)
$Ra = \frac{g\beta\Delta T L^3}{\nu a}$	Rayleight number (–)
T	temperature (°C or K)
ΔT	temperature difference (K)
U	voltage (V)
V	volume of the cube (m^3)
w	velocity of the fluid (m/s)
x'	the boundary layer length measured along the streamlines in the bottom corner region (m)

Greek symbols

α	heat transfer coefficient ($W/(m^2 K)$)
β	average volumetric thermal expansion coefficient (1/K)
δ^*	dimensionless boundary layer thickness (–)
δ	boundary layer thickness (m)
δ_f	final thickness of dimensionless boundary layer (m)
λ	thermal conductivity of the fluid (W/m K)
ν	kinematic viscosity of the fluid (m^2/s)
Θ	dimensionless temperature defined by Eq. (4)

Subscripts

1l	region 1 lateral
1c	region 1 corner
2l	region 2 lateral
2c	region 2 corner
3l	region 3 lateral
3c	region 3 corner
c	convective
f	final
n	normal
r	radiative
τ	tangential
w	wall
∞	bulk fluid

convective heat transfer from a wall-mounted single array of cubical protrusions along a wall at a wind tunnel. Nakamura et al. [17] presented the data about the cooling design of electric equipment in the form of cubes and square blocks. Culham and Yovanovich with Lee [18] calculated the thermal performance of several heat sinks using a flat plate boundary model, also for isothermal cuboids with the square root of the surface $A^{1/2}$ as the characteristic length in the form:

$Nu_{\sqrt{A}} = 3.42 + 0.524Ra_{\sqrt{A}}^{1/4}$ for cuboids with aspect ratios length/width $= 1{:}1$ and $Nu_{\sqrt{A}} = 3.89 + 0.594Ra_{\sqrt{A}}^{1/4}$ for cuboids with aspect ratios length/width $= 10{:}1$.

This paper is focused on analytical solution of simplified Navier–Stokes and Fourier–Kirchhoff equations, described natural convective heat transfer from isothermal cuboids immersed in fluid treated as unlimited space.

Obtained for cuboids of different shapes (determined by length, width and height) solution has been verified experimentally. In the experimental study we tested the same cuboid with dimensions 0.2 m $\times$ 0.1 m $\times$ 0.045 m situated in three positions: vertical I, lateral II and horizontal III. In this way the errors of measurements were for all tested positions the same.

2. The theoretical considerations

According to the surface orientation to the gravitational acceleration the cuboid was divided into three regions correlated with the heat transfer direction (Fig. 1). Region 1 is the bottom of the cuboid and it is treated as the sum of two rectangular horizontal and faced down rectangles (1l) with the surface $((b-a)a/2)$ each and eight horizontal down-faced triangles (1c) with the surface $(a^2/8)$ each. Region 2 is composed of two vertical rectangles (2l) with the surface $((b-a)c)$ each and eight vertical rectangles (2c) with the surface $(ac/2)$ each. Region 3 is the rectangular horizontal plate facing upward, created by two rectangles (3l) with the surface $((b-a)a/2)$ each and eight triangles (3c) with the surface $(a^2/8)$ each.

The mean heat transfer coefficient for the cuboid can be obtained from the energy balance ($Q = Q_1 + Q_2 + Q_3$)

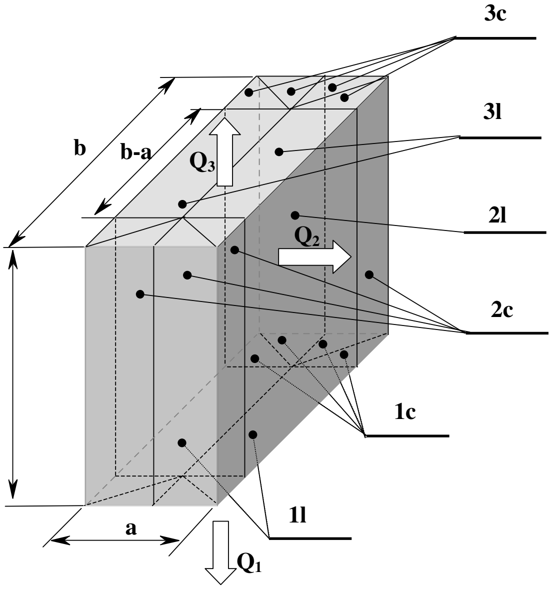

Fig. 1. The regions of the cuboid, correlated with the heat transfer phenomenon: 1—horizontal faced-down, 2—vertical, 3—horizontal faced up and subregions: l—lateral, c—corner.

by averaging heat transfer coefficients obtained for all mentioned above regions and subregions:

$$\overline{\alpha}=\frac{(b-a)a(\overline{\alpha}_{1l}+\overline{\alpha}_{3l})+a^2(\overline{\alpha}_{1c}+\overline{\alpha}_{3c})+4ac\overline{\alpha}_{2c}+2(b-a)c\overline{\alpha}_{2l}}{2(ac+ab+bc)} \quad (1)$$

Introducing the simplifying assumptions typical for the natural convection and proposed physical model such as:

- fluid is incompressible and its flow is laminar and steady,
- the flow is predominantly parallel to the control surface of heated wall, with the boundary layer develop with the distance along the surface,
- physical properties of the fluid in the boundary layer and in the undisturbed region are constant,
- temperature of the cuboid's surface (T_w) is constant,
- inertia terms, viscous dissipation and internal heat sources are neglected,
- conductive heat losses through suspension of the cuboid to the fluid is disregard in comparison with convective one,
- thickness of thermal and hydraulic boundary layers are the same

so the Navier–Stokes equations for the control space inside the boundary layer may be written for any positions of heated surface in terms:

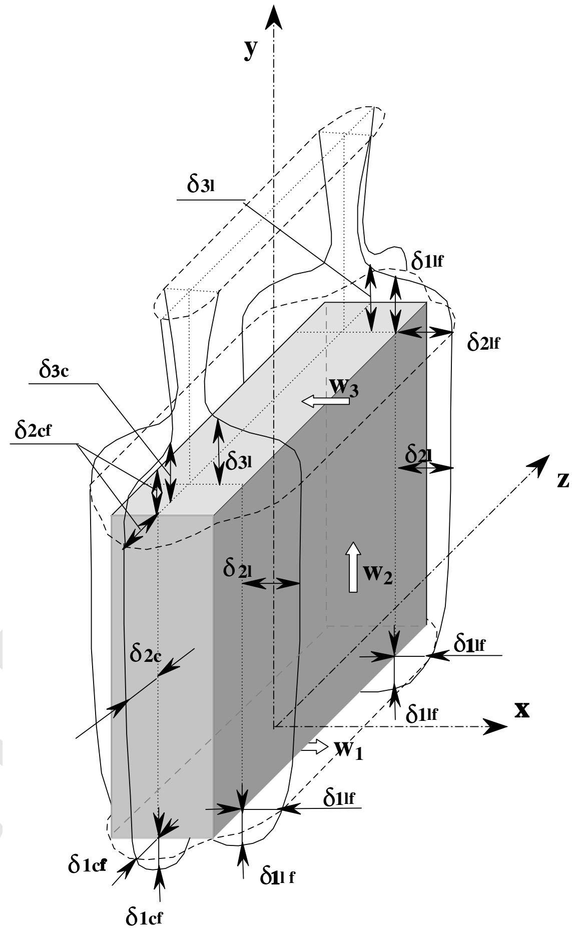

Fig. 2. The boundary layer shapes and thickness in the defined regions.

$$v\frac{\partial^2 w_\tau}{\partial n^2}+g\beta(T_\tau-T_\infty)\sin\phi-\frac{1}{\rho}\frac{\partial p}{\partial\tau}=0 \quad (2)$$

$$g\beta(T_\tau-T_\infty)\cos\phi-\frac{1}{\rho}\frac{\partial p}{\partial n}=0 \quad (3)$$

where (ϕ) is an angle of inclination of considered surface: ($\phi=0$) for the horizontal and ($\phi=\pi/2$) for vertical surface, (τ) and (n) are the tangential and normal to the fluid flow directions.

Instead of the direct form of the Fourier–Kirchhoff equation it was decided, according to Squire and Eckert [19,20], to make assumption that the temperature profile in the boundary layer is described by:

$$\Theta=\frac{T-T_\infty}{T_w-T_\infty}=\left(1-\frac{n}{\delta}\right)^2 \quad (4)$$

The quasi-analytical solution of Eqs. (1)–(3), presented in Ref. [21] in the form of the local and mean velocity in control space across the boundary layer are:

$$w_\tau = \frac{g\beta\Delta T}{\nu}\left[\frac{\mathrm{d}\delta}{\mathrm{d}\tau}\left(\frac{n^4}{12\delta^2} - \frac{2n^5}{60\delta^3} - \frac{n^2}{6} + \frac{7\delta n}{60}\right)\cos\phi + \left(-\frac{n^2}{2} + \frac{n^3}{3\delta} - \frac{n^4}{12\delta^2} + \frac{\delta n}{4}\right)\sin\phi\right], \tag{5}$$

$$\overline{w}_\tau = \frac{1}{\delta}\int_0^\delta w_\tau\,\mathrm{d}y = \frac{g\beta\Delta T\delta^2}{\nu}\left(\frac{\mathrm{d}\delta}{\mathrm{d}\tau}\frac{\cos\phi}{72} + \frac{\sin\phi}{40}\right) \tag{6}$$

The change in mass flow intensity in control surface across the boundary layer (A) is

$$\mathrm{d}m = \mathrm{d}(A\overline{w}_\tau\rho) \tag{7}$$

The amount of the heat necessary to create this change in mass flux is

$$\mathrm{d}Q = \Delta i\,\mathrm{d}m = \rho c_\mathrm{p}(\overline{T - T_\infty})\,\mathrm{d}(A\overline{w}_\tau) \tag{8}$$

Substitution of the mean value of the temperature

$$(\overline{T - T_\infty}) = \frac{1}{\delta}\int_0^\delta \Delta T\left(1 - \frac{n}{\delta}\right)^2 \mathrm{d}n = \frac{\Delta T}{3} \tag{9}$$

gives

$$\mathrm{d}Q = \frac{\rho C_\mathrm{p}\Delta T\,\mathrm{d}(A\overline{w}_\tau)}{3} \tag{10}$$

The heat flux described by Eq. (9) may be compared to the heat flux determined by Newton's Eq. (10):

$$\mathrm{d}Q = \alpha\Delta T\,\mathrm{d}S = -\lambda\left(\frac{\partial\Theta}{\partial n}\right)_{n=0}\Delta T\,\mathrm{d}S, \tag{11}$$

where ($\mathrm{d}S$) is the control surface of the heating surface.

From simplifying assumption of the temperature profile inside the boundary layer (4), the dimensionless temperature gradient on the heated surface may be evaluated as:

$$\alpha = \lambda\left(\frac{\partial\Theta}{\partial n}\right)_{n=0} = -\frac{2\lambda}{\delta} \tag{12}$$

Comparing the heat flux emitted by the wall surface with the heat flux transported by the fluid one can obtain:

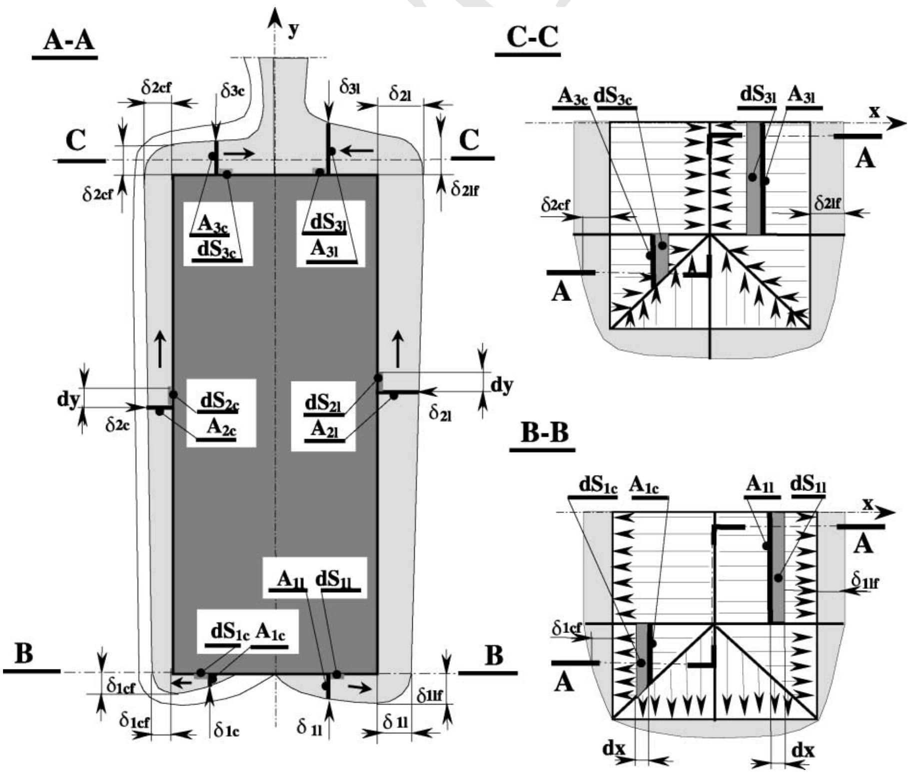

Fig. 3. Three sections of tested cuboids with boundary layers: A-A—longitudinal offset section, where the left section was made through the corner subregions, the right section -through the lateral ones; B-B—cross-section through boundary layer below down faced surface of the bottom with stream lines patterns; C-C—cross-section through boundary layer above up faced surface of the top of the cuboid with stream lines patterns.

$$\frac{1}{6}\frac{\rho c_p \delta}{\lambda}\,\mathrm{d}(A\overline{w}_\tau) = \mathrm{d}S \tag{13}$$

2.1. Detailed solution for the region 1

The phenomenon in this region of the cuboid is well known case of the convective heat transfer from down-faced horizontal plate. For the case of rectangles (Fig. 3 the cross-section B-B) streamlines are parallel to each other. The boundary layer arises from the axes of symmetry and diagonals of the surface. According to the patterns of the stream lines shown on the dawn faced horizontal rectangular plate view (Fig. 3 B-B), one can distinguished two sub regions: first, with two rectangles (1l) and the second one, with eight triangles (1c). For the first of them the control surface A has the same width independently on the position along the boundary layer on the plate. For the triangles (1c) the width of the control surfaces A are the function of not only the thickness of boundary layer (δ) but also the distance from the edges.

2.1.1. Bottom lateral side

For the rectangles the control surfaces can be defined as (Fig. 3 B-B):

$$A_{11} = (b-a)\delta_{11} \quad \text{and} \quad \mathrm{d}S_{11} = (b-a)\,\mathrm{d}x \tag{14}$$

and from the mean velocity of the fluid flow along the streamlines (6) is:

$$\overline{w}_x = \frac{1}{\delta_{11}}\int_0^{\delta_{11}} w_x\,\mathrm{d}y = \frac{g\beta\Delta T\delta_{11}^2}{72\nu}\frac{\mathrm{d}\delta_{11}}{\mathrm{d}x} \tag{15}$$

Substituting (14) and (15) into (13) one obtain equation:

$$3\delta_{11}^3\left(\frac{\mathrm{d}\delta_{11}}{\mathrm{d}x}\right)^2 + \delta_{11}^4\frac{\mathrm{d}^2\delta_{11}}{\mathrm{d}x^2} = \frac{432\left(\frac{a}{2}\right)^3}{Ra_{a/2}} \tag{16}$$

where

$$Ra_{a/2} = \frac{g\beta\Delta T\left(\frac{a}{2}\right)^3}{\nu a} \tag{17}$$

Eq. (16) has the solution in the form of boundary layer thickness:

$$\delta_{11} = \frac{4.478\left(\frac{a}{2}\right)^{3/5}x^{2/5}}{Ra_{a/2}^{1/5}} \tag{18}$$

and next, according to the Eq. (12), one can calculate the mean value of the heat transfer coefficient for this region:

$$\overline{\alpha_{11}} = \frac{2}{a}\int_0^{a/2}\frac{2\lambda}{\delta_{11}}\,\mathrm{d}x = 0.744\lambda\frac{Ra_{a/2}^{1/5}}{a/2} \tag{19}$$

2.1.2. Bottom corner side

The streamlines below the defined above triangular corner's regions (1c) are directed perpendicularly to the edges of the plate along the x or z-coordinate (Fig. 3 "B-B"). The velocity of the fluid w_x and w_z is described by the same function due to symmetry of the phenomenon.

The control surfaces for these rectangular triangles are defined as:

$$A_{1c} = z\delta_{1c} \quad \text{and} \quad \mathrm{d}S_{1c} = z\,\mathrm{d}x \tag{20}$$

and the mean velocity value obtained from (6) is:

$$\overline{w}_x = \frac{g\beta\Delta T\delta_{1c}^2}{72\nu}\frac{\mathrm{d}\delta_{1c}}{\mathrm{d}x} \tag{21}$$

Writing the Eq. (13) for this surfaces in the form:

$$\frac{1}{6}\frac{\rho c_p\delta_{1c}}{\lambda}\,\mathrm{d}(A_{1c}\overline{w}_x) = \mathrm{d}S_{1c} \tag{22}$$

and

$$\frac{1}{432}\frac{Ra_{a/2}^{1/5}}{\left(\frac{a}{2}\right)^3}\delta_{1c}\frac{\mathrm{d}}{\mathrm{d}x}\left(\delta_{1c}\frac{\mathrm{d}\delta_{1c}}{\mathrm{d}x}\right) = 1 \tag{23}$$

one can find the solution:

$$\delta_{1c} = \frac{4.478\left(\frac{a}{2}\right)^{3/5}x^{2/5}}{Ra_{a/2}^{1/5}} \tag{24}$$

In this subregion the fluid flow starts from the hypotenuse of each rectangular triangle and goes perpendicularly to the edges so the length of boundary layer along streamlines can be described by: ($x' = (a/2) - x$) (Fig. 4) which changes from $x' = a/2$ for $z = 0$ to $x' = 0$ for $z = a/2$. Taking it into account in Eq. (24) one can obtain the boundary layer thickness in the form:

$$\delta_{1c} = \frac{4.478\left(\frac{a}{2}\right)^{3/5}\left(\frac{a}{2}-x\right)^{2/5}}{Ra_{a/2}^{1/5}} \tag{25}$$

and next the mean heat transfer coefficient from this regions:

$$\overline{\alpha_{1c}} = \frac{1}{S}\int_S\frac{2\lambda}{\delta_{1c}}\,\mathrm{d}S = \frac{16\lambda}{a^2}\frac{Ra_{a/2}^{1/5}}{4.478\left(\frac{a}{2}\right)^{3/5}}\int_0^{a/2}\int_{((a/2)-z)}^{a/2}\left(\frac{a}{2}-x\right)^{-2/5}\mathrm{d}x\,\mathrm{d}z = 0.93\lambda\frac{Ra_{a/2}^{1/5}}{\frac{a}{2}} \tag{26}$$

2.2. Solution for the region 2

The heat transfer in this region can be treated as the well-known case of natural convection from isothermal vertical surface. Instead of the typical vertical plates for the cuboid the boundary layer thickness is not equal zero at the bottom edge but is equal to the final

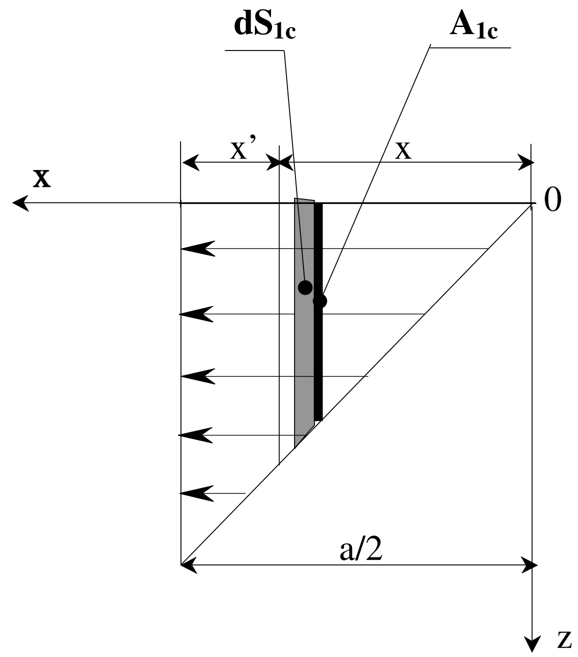

Fig. 4. Enlarged fragment of the presented on Fig. 3 B-B the bottom corner subregion (1c) with the explanation of fluid flow model and control surfaces definitions.

boundary layers thickness from the previous subregion (δ_{1lf}) or (δ_{1cf}) (see Figs. 2 and 3 A-A). Because the values of final boundary layers thickness differs from each other this was the reason why the region 2 has been divided into two sub regions: the vertical lateral (2l) and corner (2c) one. For the first of them (2l) the initial values of boundary layer thickness is constant (Eq. (18) for $x = a/2$) but for region (2c) it is the function of the distance from the corner of the cuboid (Eq. (24)).

Both vertical lateral side (2l) and corner side (2c) have the control surfaces defined as:

$$A_{2l} = y\delta_{2l} \quad \text{and} \quad \mathrm{d}S_{2l} = y\,\mathrm{d}y \tag{27}$$

and the mean velocity value obtained from (6):

$$\overline{w}_y = \frac{g\beta\Delta T\delta_{2l}^2}{40\nu} \tag{28}$$

Comparing the heat flux emitted by the heated wall with the heat flux transported by the fluid one can obtain the equation:

$$\frac{1}{240}\frac{Ra_c}{c^3}\frac{\delta_{2l}}{y}\frac{\mathrm{d}}{\mathrm{d}y}(y\delta_{2l}^3) = 1 \tag{29}$$

which solution is the boundary layer thickness

$$\delta_{2l} = \left(\frac{240c^3}{Ra_c}\frac{4}{7}y\right)^{1/4} \tag{30}$$

2.2.1. The vertical lateral side

For estimating the mean heat transfer coefficient for the subregion (2l) one should take the length of the boundary layer as $(c + \delta_{1lf})$ and then integrating borders from $(-\delta_{1lf})$ to (c), where (δ_{1lf}) is the final thickness of boundary layer from bottom in lateral region (18) for $(x = a/2 = \text{const.})$, described by equation:

$$\delta_{1lf} = \frac{4.478\left(\frac{a}{2}\right)^{3/5}\left(\frac{a}{2}\right)^{2/5}}{Ra_{a/2}^{1/5}} = \frac{2.239a}{Ra_{a/2}^{1/5}} \tag{31}$$

Introduction Eq. (30) into (12) leads to the local and next the mean heat transfer coefficient from this region

$$\overline{\alpha}_{2l} = \frac{2\lambda}{c}\int_{-2.239a/Ra_{a/2}^{1/5}}^{c}\left(\frac{4}{7}\frac{240c^3}{Ra_c}\right)^{-1/4} y^{-1/4}\,\mathrm{d}y \tag{32}$$

and then

$$\overline{\alpha}_{2l} = 0.779\lambda\frac{Ra_c^{1/4}}{c}\left[1 + \left(\frac{2.239a}{Ra_{a/2}^{1/5}c}\right)^{3/4}\right] \tag{33}$$

2.2.2. The vertical corner region

For estimating the mean heat transfer coefficient from the subregion (2c) one should take the length of boundary layer as $c + \delta_{1lc}$ and then integrating borders from $(-\delta_{1cf})$ to (c), where (δ_{1cf}) is the final thickness of boundary layer from bottom in the corner region. Due to the symmetry of the phenomenon $(x = z)$.

Accordingly to Eq. (25) for $x = a/2$ and $z' = (a/2) - z$ the final value of the boundary layer thickness for this sub region is:

$$\delta_{1cf}(z) = \frac{4.478\left(\frac{a}{2} - z\right)^{3/5}\left(\frac{a}{2}\right)^{2/5}}{Ra_{a/2}^{1/5}} \tag{34}$$

The mean heat transfer coefficient from the regions (2c) is described by the equation:

$$\overline{\alpha}_{2c} = \frac{1}{a/2}\int_0^{a/2}\left[\frac{1}{c}\int_{-\delta_{1cf}(z)}^{c}\frac{2\lambda}{\left(\frac{4}{7}\frac{240c^3}{Ra_c}y\right)^{1/4}}\,\mathrm{d}y\right]\mathrm{d}z$$
$$= 0.779\lambda\frac{Ra_c^{1/4}}{c} + 0.984\lambda\frac{Ra_c^{1/4}}{Ra_{a/2}^{3/20}}\frac{a^{3/4}}{c^{7/4}} \tag{35}$$

2.3. Solution for the region 3

Region 3 is known case of the heat transfer from the horizontal rectangular plate facing upward, for example [22]. The stream lines are shown schematically on Fig. 3 (cross-section C-C). In this region the rectangular plate should also be considered as the sum of two rectangles and eight triangles and the heat transfer is now influenced by boundary layer formed on the bottom and next vertical sides of the cuboid. Integration of the heat transfer coefficient has to take into account the final boundary layer thickness $\delta_{2\mathrm{lf}}$ and $\delta_{2\mathrm{cf}}$.

2.3.1. The upper lateral region

The heat transfer in this region is influenced by the final boundary layer thickness from the lateral vertical side (2lf). The boundary layer thickness obtained for lateral top regions in the form [22]:

$$\delta_{3\mathrm{l}} = \frac{4.478\left(\frac{a}{2}\right)^{3/5} x^{2/5}}{Ra_{a/2}^{1/5}} \tag{36}$$

should be now integrated from $(-\delta_{2\mathrm{lf}})$ to $(a/2)$, where final thickness of boundary layer $(\delta_{2\mathrm{lf}})$ can be calculated from (30) for $(y = c + \delta_{1\mathrm{lf}})$:

$$\begin{aligned}\delta_{2\mathrm{lf}} &= \delta_{2\mathrm{l}}(y = c + \delta_{1\mathrm{lf}}) \\ &= \left(\frac{4}{7}\frac{240c^3}{Ra_c}\right)^{1/4}\left(c + \frac{2.239a}{Ra_{a/2}^{1/5}}\right)^{1/4}\end{aligned} \tag{37}$$

Then one can obtain the mean heat transfer coefficient:

$$\begin{aligned}\overline{\alpha}_{3\mathrm{l}} &= \frac{1}{a/2}\int_{-\delta_{2\mathrm{lf}}}^{a/2} \frac{2\lambda}{\delta_{3\mathrm{l}}}\,\mathrm{d}x \\ &= 0.744\lambda \frac{Ra_{a/2}^{1/5}}{\frac{a}{2}}\left\{1 + \frac{\left[\frac{4}{7}\frac{240c^3}{Ra_c}\left(c + \frac{2.239a}{Ra_{a/2}^{1/5}}\right)\right]^{3/20}}{\left(\frac{a}{2}\right)^{3/5}}\right\}\end{aligned} \tag{38}$$

2.3.2. The upper corner region

The final boundary layer thickness from (2cf) subregion is the function of coordinates (x) or (z), so for the upper triangles the Eq. (37) should be transformed as (34) to:

$$\begin{aligned}\delta_{2\mathrm{cf}} &= \delta_{2\mathrm{c}}(y = c + \delta_{1\mathrm{cf}}) \\ &= \left(\frac{4}{7}\frac{240c^3}{Ra_c}\right)^{1/4}\left(c + \frac{4.478\left(\frac{a}{2} - x\right)^{3/5}\left(\frac{a}{2}\right)^{2/5}}{Ra_{a/2}^{1/5}}\right)^{1/4}\end{aligned} \tag{39}$$

and the mean value of the heat transfer coefficient for the regions (3c) can be described as:

$$\begin{aligned}\overline{\alpha_{3\mathrm{c}}} &= \frac{4}{a^2}\int_{-\delta_{2\mathrm{cf}}(x)}^{a/2}\left(\int_{-\delta_{2\mathrm{cf}}(z)}^{a/2}\frac{2\lambda}{\delta_{3\mathrm{c}}}\,\mathrm{d}x\right)\mathrm{d}z \\ &= 0.744\lambda\frac{Ra_{a/2}^{1/5}}{a/2}\left[1 + \frac{\left(\frac{4}{7}\frac{240c^3}{Ra_c}\right)^{3/20}}{\left(\frac{a}{2}\right)^{3/5}}\left(c + \frac{1.477a}{Ra_{a/2}^{1/5}}\right)^{3/20}\right]\end{aligned} \tag{40}$$

where the last integrating in (40) was replaced by the mean value without considerable inaccuracy.

2.4. The Nusselt–Rayleigh relation for the isothermal cuboid

Substituting (19), (26), (32), (34), (37) and (39) to the Eq. (1) the mean heat transfer coefficient for the cube can be estimated. Majority of the heat transfer analyses are based on correlations Nusselt number versus Rayleigh number in the form:

$$Nu = CRa^n \tag{41}$$

Nusselt and Rayleigh numbers are defined as:

$$Nu_L = \frac{\overline{\alpha}L}{\lambda} \quad \text{and} \quad Ra_L = \frac{g\beta\Delta TL^3}{\nu a} \tag{42}$$

with L as the characteristic linear dimension.

On the base of our own and other investigators data we have been considered the linear characteristic length choice. We taken into account height of the cuboid (c), the boundary layer length $(a + c)$, the square root of the surface $(\sqrt{A})$ and the length defined by:

$$L = \frac{6V}{F} = \frac{3abc}{ab + ac + bc} \tag{43}$$

where V is the volume and F is cuboid's surface,

Ultimately we have chosen the characteristic length (43) and substituting:

$$\begin{aligned}Ra_{a/2} &= Ra_L\left(\frac{ab + ac + bc}{6bc}\right)^3 \quad \text{and} \\ Ra_c &= Ra_L\left(\frac{ab + ac + bc}{3ab}\right)^3\end{aligned} \tag{44}$$

the $Nu_L(Ra_L)$ relation can be described in form:

$$Nu_L = XRa_L^{1/5} + YRa_L^{1/4} \tag{45}$$

where

$$\begin{aligned}X = \frac{a(6bc)^{2/5}}{4(ab + ac + bc)^{7/5}}&\left\{2.976b + 0.372a\right. \\ &+ \frac{1.488}{\left(\frac{a}{2}\right)^{3/5}}\left[\frac{4}{7}\frac{240c^3}{Ra_L\left(\frac{ab+ac+bc}{3ab}\right)^3}\right]^{3/20}\left[(b - a)\right. \\ &\times\left(c + \frac{2.239a}{Ra_L^{1/5}\left(\frac{ab+ac+bc}{6bc}\right)^{3/5}}\right)^{3/20} \\ &\left.\left. + a\left(c + \frac{1.477a}{Ra_L^{1/5}\left(\frac{ab+ac+bc}{6bc}\right)^{3/5}}\right)^{3/20}\right]\right\}\end{aligned} \tag{46}$$

and

$$Y = \frac{c(3ab)^{1/4}}{2(ab+ac+bc)^{5/4}}\left[1.558(a+b) + \frac{3.936a\left(\frac{a}{c}\right)^{3/4} + 1.558(b-a)\left(2.239\frac{a}{c}\right)^{3/4}}{Ra_L^{3/20}\left(\frac{ab+ac+bc}{6bc}\right)^{9/20}}\right] \tag{47}$$

The Eq. (45) with coefficients (46) and (47) has the universal form and does not depend on the cuboids position—it makes allowance for the influence both the horizontal and vertical sides of the block, which are usually described separately with the exponents: 1/5 and 1/4 accordingly.

3. Experimental apparatus and procedure

Experiment was conducted in the air in a vessel with the volume of 1.5 m^3. The tested cuboid was made of polished aluminium and had the dimensions: 0.2, 0.1, and 0.045 m. It was hanged in the vessel with the use of two nylon wires which was 0.5 mm thick in three positions of cuboid's orientation: I-vertical-for height $c = 0.2$ m, II-lateral-for height $c = 0.1$ m and III-horizontal-for height $c = 0.045$ m.

The electric heater (power transistors) was placed inside the cuboid. Heat flux from the surface of the block to surrounding test fluid was transferred mainly by laminar convection and partially by radiation. Six thermocouples were used to measure the surface temperature, one on the each side of the cube. They were soldered into holes of aluminium with the tips of about 0.001 m. Four thermocouples were used to measure the bulk temperature (T_∞) of the fluid (air) at different levels in the tank. The inaccuracy of the temperature measurement did not exceed ±0.1 K. Establishing of different steady states was made by a cooling system located at the top of the vessel. During the experimental runs the surface temperatures of the cube, bulk temperature of the fluid and the voltage (U) and current of the heater inside the cuboid (I) were measured. All these data were recorded during established steady states. The time of obtaining a thermal equilibrium and performing of experimental studies was about 6 h for one experimental point.

4. Experimental results and analysis

In steady-state conditions the heat balance at the exterior surface requires that the rate of heat gain is equal to the rate of heat loss. This balance must be maintained between the heat flux form inside the cuboid and the convective and radiative losses from the external surfaces to the air. The only source of heat flux form inside the cube was the electric power of the heater. Because thin nylon wires eliminated the solid metal support of the cuboid, the heat losses by conduction through the support have not been taken into account.

A series of experimental runs in air according to the apparatus described above was made in three configurations of the cube. For every steady-state point the temperature of the cuboid's sides (T_w), the bulk fluid (T_∞) and the electric power of the hater (UI) was saved by computer system.

Then the Nu and Rayleigh numbers were estimated as:

$$Nu_L = \frac{\alpha L}{\lambda}, \quad Ra_L = \frac{g\beta(T_w - T_\infty)L^3}{va} \tag{48}$$

where α was calculated from the Newton's law:

$$\alpha = \frac{\dot{Q}_c}{F(T_w - T_\infty)} = \frac{UI - \dot{Q}_r}{F(T_w - T_\infty)} \tag{49}$$

and $\dot{Q}_r$ is the radiative heat flux form the cuboids surface.

All measurements were counted out with the least square method using three proposed characteristic lengths. The first one was the height of the cuboid, what is the equivalent of the characteristic linear dimension used for the vertical plates. It gave the $Nu(Ra)$ relation (Fig. 5):

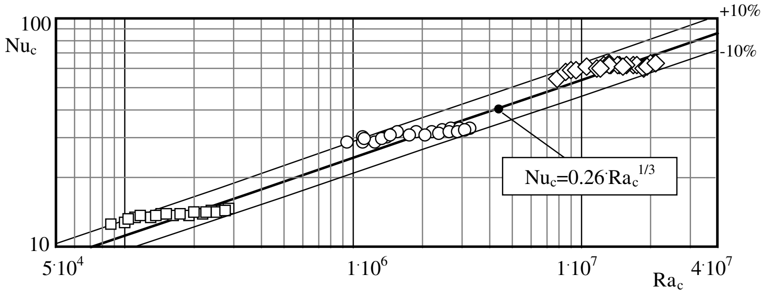

Fig. 5. Experimental results in comparison with theoretical values for three positions of the tested cuboid: (□) position I, (◯) position II, (◇) position III in the logarithmic scale with the height of the cuboid as the characteristic linear dimension.

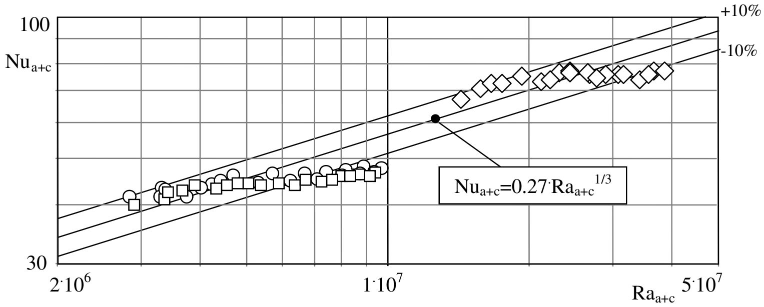

Fig. 6. Experimental results in comparison with theoretical values for three positions of the tested cuboid: (□) position I, (◯) position II, (◇) position III in the logarithmic scale with the sum of height and length of the cuboid as the characteristic linear dimension.

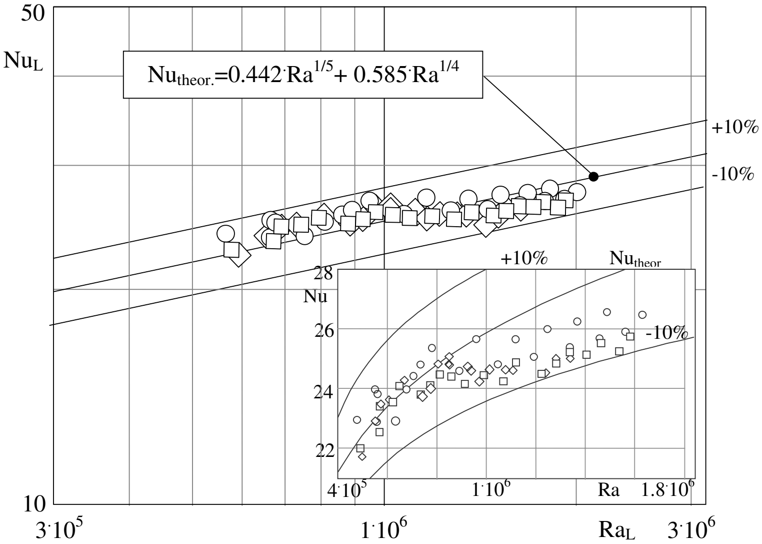

Fig. 7. Experimental results in comparison with theoretical values for three positions of the tested cuboid: (□) position I, (◯) position II, (◇) position III in the logarithmic scale with enlarged detail in non-logarithmic scale.

$$Nu_c = 0.26Ra_c^{1/3} \quad (50)$$

The second linear dimension was the length of the boundary layer, equal the sum of the length and height of the cuboid $(a/2 + c + a/2)$. Then obtained criterial relation was similar to (50) (Fig. 6):

$$Nu_{a+c} = 0.27Ra_{a+c}^{1/3} \quad (51)$$

Ultimately the characteristic length $(L = 6V/F)$ (43) turned out the most useful and allowed performing all experimental result, apart from the position of the cuboid (Fig. 7). The obtained relation can be drawn in form

$$Nu_L = 1.596Ra_L^{1/5} \text{ or } Nu_L = 0.818Ra_L^{1/4} \quad (52)$$

For the tested cuboid the Nu_l (Ra_l) relations, obtained from (45) with (46) and (47) are:

$$Nu_L = 0.442Ra_L^{1/5} + 0.585Ra_L^{1/4} \quad (53)$$

what is adequate to:

$$Nu_L = 1.61Ra_L^{1/5} \text{ or } Nu_L = 0.807Ra_L^{1/4} \quad (54)$$

that agrees well with (52) within ±1.35%.

5. Conclusions

The natural convection heat transfer in unlimited space from isothermal cuboid has been theoretically and experimentally investigated. Obtained correlation Nu_L (Ra_L) allows calculating the convective heat transfer intensity for the cuboids with any dimensions and positions regarding the direction of gravity acceleration. The solutions are in good agreement with experimental results presented in this paper and would be included into prepare energy balance objects in the form of cuboid.

References

[1] T. Fujii, H. Imura, Natural-convection heat transfer from a plate with arbitrary inclination, Int. J. Heat Mass Transfer 15 (1972) 755–767.

[2] F. Restrepo, L.R. Glicksman, The effect of edge conditions on natural convection from a horizontal plate, Int. J. Heat Mass Transfer 17 (1974) 135–142.

[3] I.P. Warneford, D.E. Fussey, Natural convection from a constant-heat-flux inclined flat plate, in: Fifth International Heat Transfer Conference, 1974.

[4] J.V. Clifton, A.J. Chapman, Natural-convection on a finite-size horizontal plate, Int. J. Heat Mass Transfer 12 (1969) 1573–1584.

[5] S.N. Singh, R.C. Birkebak, R.M. Drake Jr., Laminar free convection heat transfer from downward-facing horizontal surfaces of finite dimensions, Prog. Heat Mass Transfer 2 (1969) 87–98, according to R.E. Faw and T.A. Dullforce.

[6] T. Schulenberg, Natural convection heat transfer below downward-facing horizontal surfaces, Int. J. Heat Mass Transfer 28 (1985) 467–477.

[7] D.E. Fussey, I.P. Warneford, Free convection from a downward facing inclined plate, Int. J. Heat Mass Transfer 21 (1978) 119–126.

[8] T. Fujii, H. Honda, I. Morioka, A theoretical study of natural convection heat transfer from downward-facing horizontal surfaces with uniform heat flux, Int. J. Heat Mass Transfer 16 (1973) 611–627.

[9] T. Aihara, Y. Yamada, S. Endo, Free convection along the downward-facing surface of a heated horizontal plate, Int. J. Heat Mass Transfer 15 (1972) 2535–2549.

[10] T. Schulenberg, Natural convection heat transfer to liquid metals below downward facing horizontal surfaces, Int. J. Heat Mass Transfer 27 (1984) 433–441.

[11] E. Radziemska, W.M. Lewandowski, Heat transfer by natural convection from isothermal downward-facing horizontal round plate, Appl. Energy 68 (2001) 347–366.

[12] W.M. Lewandowski, E. Radziemska, Free convective heat transfer from isothermal vertical round plate, Appl. Energy 68 (2001) 347–366.

[13] J.R. Culham, M.M. Yovanovich, P. Teertstra, C.-S. Wang, Simplified analytical models for forced convection heat transfer from cuboids of arbitrary shape, EEP-Vol. 26-1, Advances in Electronic Packaging, vol. 1, ASME, 1999.

[14] D.J. Cha, S.S. Cha, Three-dimensional natural convective flow around two interacting isothermal cubes, Int. J. Heat Mass Transfer 38 (13) (1995) 2343–2352.

[15] M.M., Yovanovich, Compact models for conductive and convective heat transfer in microelectronic applications for the new millenium, in: 34th National Heat Transfer Conference, August 2000.

[16] E.R. Meinders, T.H. van der Meer, K. Hanjalič, Local heat transfer from an array of wall-mounted cubes, Int. J. Heat Mass Transfer 41 (2) (1998) 335–346.

[17] H. Nakamura, T. Igaroshi, T. Tsutsui, Local heat transfer around a wall-mounted cube in the turbulent boundary layer, Int. J. Heat Mass Transfer 44 (2001) 3385–3395.

[18] J.R. Culham, M.M. Yovanovich, S. Lee, Thermally modeling isothermal cuboids and rectangular sinks cooled by natural convection, IEEE Trans. Components, Packaging Manuf. Technol., Part A 18 (3) (1995).

[19] H.B. Squire, in: S. Goldstein (Ed.), Modern Developments in Fluid Dynamics, Oxford Clarendon Press, 1938, or in New York, Dover 1965.

[20] E.R.G. Eckert, Heat and Mass Transfer, Mc. Graw-Hill Book Company, New York, 1959, p. 312.

[21] W.M. Lewandowski, Natural convection heat transfer from plates of finite dimensions, Int. J. Heat and Mass Transfer 34 (3) (1991) 875–885.

[22] W.M. Lewandowski, E. Radziemska, M. Buzuk, H. Bieszk, Free convection heat transfer and fluid flow structures above horizontal rectangular plates, Appl. Energy 66 (2000) 177–197.